Limitations of perturbative coupled-cluster approximations for highly accurate investigations of ${\rm Rb_2}^+$

Jan Schnabel, Lan Cheng, and Andreas Köhn

¹⁾Institute for Theoretical Chemistry and Center for Integrated Quantum Science and Technology, University of Stuttgart, 70569 Stuttgart, Germany

²⁾Department of Chemistry, The Johns Hopkins University, Baltimore, Maryland 21218, United States

(*Electronic mail: schnabel@theochem.uni-stuttgart.de)

(*Electronic mail: lcheng24@jhu.edu)

(*Electronic mail: koehn@theochem.uni-stuttgart.de)

(Dated: August 17, 2021)

We reveal limitations of several standard coupled-cluster (CC) methods with perturbation-theory based noniterative or approximate iterative treatments of triple excitations when applied to the determination of highly accurate potential energy curves (PECs) of ionic dimers, such as the $X^2\Sigma_p^+$ electronic ground state of Rb₂⁺. Such computations are of current interest for the understanding of ion-atom interactions in the ultracold regime. We demonstrate that these CC methods lead to an unphysical long-range barrier for the Rb2+ system. The barrier is small but spoils the long-range behavior of the PEC. The effect is also found for other X_2^+ systems, like X = Li, Na, and K. Calculations using a flexible framework for obtaining leading perturbative triples corrections derived using an analytic CC singles and doubles (CCSD) energy derivative formulation demonstrate that the origin of this problem lies in the use of \hat{T}_3 amplitudes obtained from approximate CC singles, doubles and triples (CCSDT) amplitude equations. It is shown that the unphysical barrier is related to a symmetry instability of the underlying Hartree-Fock mean-field solution leading to orbitals representing two +0.5-fold charged ions in the limit of separated fragments. This in turn leads to a wrong 1/R asymptote of the interaction potential computed by perturbation-based coupled-cluster approximations. Physically meaningful perturbative corrections in the long-range tail of the PEC may instead be obtained using symmetry-broken reference determinants.

I. INTRODUCTION

The understanding and the gain of control of interacting neutral atoms in the ultracold quantum regime has grown substantially over the past decades. The achievements, to mention only a few of them, reach from Bose-Einstein condensation (BEC)¹, over Rydberg systems^{2–4} to creating and controlling ultracold molecules^{5–7}. While for neutral atoms reaching the ultracold quantum scattering regime (i.e. s-wave collision regime) is nowadays well established, it is still a non-trivial challenge to reach the quantum scattering regime for hybrid ion-atom systems due to more stringent temperature requirements⁸. This is extremely desirable as hybrid ion-atom systems are expected to pave the way for novel experiments, phenomena and applications

– among others the precision measurements of ionatom collision parameters and associated molecular potentials^{9–11}.

Novel experimental approaches have been proposed recently in Refs. 12,13. Here the ion-atom interaction for a core of a giant Rydberg atom immersed in a BEC of ⁸⁷Rb leading to a temperature environment below a microkelvin has been studied. In principle, the experimental accuracy achievable with this approach is in the MHz – $(= \mathcal{O}(10^{-5}\,\mathrm{cm}^{-1}) -)$ domain with a characteristic range of the ion-atom interaction (for Rb) of $R^* = \sqrt{\mu C_4} \approx 5000\,\mathrm{a_0}^8$.

These pilot experiments, see e.g. Ref. 12 and references therein, aim at entering the s-wave scattering regime and eventually studying the ro-vibrational structure (of, e.g., the threshold

bound states) and charge-transfer processes of Rb2⁺. Therefore, highly accurate potential energy curves (PECs) are needed as a starting point for subsequent studies of corresponding properties related to design and performance of these experiments. The PECs have to be accurate not only in the long-range region (up to $R_{\infty} = R^* \approx 5000\,a_0$ to investigate scattering effects sufficiently), but also in the short-range region (to provide an accurate insight into the rovibrational structure). The long-range part of the interaction potential between an S-state ion and an S-state atom in the electronic ground state is given by⁸

$$V_{\rm ion-atom}^{\rm LR} \approx -\frac{C_4^{\rm ind}}{R^4} - \frac{C_6^{\rm ind}}{R^6} - \frac{C_6^{\rm disp}}{R^6} + \dots$$
 (1)

The $C_4^{\rm ind}$ and $C_6^{\rm ind}$ terms describe the interaction between the charge of the ion and the induced electric dipole (quadrupole) moment of the atom, while the C_6^{disp} dispersion term represents the interaction between instantaneous dipole-induced dipole moments of the ion and atom arising due to quantum fluctuations⁸. Patil and Tang approximately evaluated multipolar polarizabilities and dispersion coefficients of homonuclear and heteronuclear interactions of both alkali and alkaline earth atoms and ions, respectively in Ref. 14. This can be further used for models studying reactive collisions, cf. e.g. Refs. 15,16. However, using approximate values for the dispersion coefficient might turn out to be insufficient for predictions to guide novel experiments. It is thus of significant interest to obtain accurate PECs using *ab-initio* calculations.

Theoretical investigations of X_2^+ systems (with X = Li, Na, K, Rb) $^{17-23}$ have been reported earlier. The electron affinity equation-of-motion coupled-cluster (EA-EOM-CC) method with scalar-relativistic effects included via the Douglas-Kroll-Hess method has been used recently $^{21-23}$ for computations on the Li_2^+ , Na_2^+ and K_2^+ systems yielding satisfactory agreement with available experimental data. As perhaps the only example aiming at high accuracy, Tomza *et al.* reported a scheme for obtaining a PEC of Li_2^+ from relativistic coupled-cluster (CC) calculations 11 . This approach demonstrated that highly accurate *ab initio* results can be used to predict bounds for the ion-atom scattering length. Among many other studies revealing the power of

ab initio theory to predict or to confirm experimental findings to high accuracy, recent work on Mg₂ in Ref. 24 showed the potential of coupled-cluster theory to accurately describe weakly bound systems. The authors were able to compute the 19 vibrational levels of the X $^1\Sigma_g^+$ state to an accuracy of $\sim 1\,\mathrm{cm}^{-1}$ compared to 14 experimentally measured term energies, giving thus useful hints to the experimental detection of the further so far unresolved levels.

To the best of our knowledge there are no examples on highly accurate computations of Rb2+. Therefore, our efforts originally aimed at a first high accuracy calculation of PECs for homonuclear molecular ions containing heavier alkali metal species using an additivity scheme as laid out in Section II. While the good performance of several CC variants, such as the completely renormalized CC theory, in reproducing CCSDT and CCSDTQ PECs for Be₂ has been demonstrated recently²⁵, our calculations for Rb2+ revealed some non-trivial subtleties in CC methods with noniterative and approximate iterative treatment of triple excitations including the coupled-cluster singles and doubles augmented with a noniterative triples correction [CCSD(T)] method, – the 'gold standard' of quantum chemistry. The corresponding theoretical basics are outlined in Sec. III. As shown in Sec. IV, this problem leads to an unphysical barrier in the long-range region of the PEC. The present paper thus is focused on understanding and solving this problem. In Sec. V the problem is analyzed and attributed to a dominant contribution of the Fockian in the corresponding equations of these approximate treatments of triple excitations. We show that physically meaningful perturbative corrections in the long-range can be obtained using symmetry-broken reference determinants. Moreover, we present an alternative approach with approximate treatment of triple excitations to obtain high accuracy and simultaneously avoiding the long-range problem to extract valuable properties such as dispersion coefficients. Finally, Section VI gives a summary and an outlook.

II. COMPUTATIONAL ASPECTS

High-accuracy quantum-chemical calculations of atomic and molecular energies often rely on additivity schemes.^{26–31} Here it is assumed that the Hartree-Fock reference energy and the CCSD(T) correlation contribution, both extrapolated to the complete basis-set (CBS) limit, form a good basis to add higher-level correlation contributions, i.e. those beyond CCSD(T) such as CCSDT, CCSDT(Q), etc., and higher-order relativistic effects on top to finally obtain the total electronic energy to the highest possible accuracy. Note that for PECs involving bond cleavage CCSD(T) is expected to fail and thus not a good base whereupon to build additivity schemes. However, for the ground state of Rb₂⁺ this is unproblematic since it is a single reference system for the entire range of interatomic distances. For this we expect CCSD(T) to work well, even though it has been noted in Refs. 32,33 that some CC variants used in combination with open-shell UHF or ROHF references are not guaranteed to perform as well as for closed-shell references.

The HF and CC calculations were performed either using the small-core effective core potential (scECP) ECP28MDF from Ref.³⁴, where the $4s^24p^65s^1$ electrons of Rb are treated explicitly and all the others are modelled via a scalar-relativistic pseudopotential (PP), or using the all-electron spinfree exact two-component theory in its one-electron variant (SFX2C-1e)^{35,36} to treat scalar-relativistic effects. We can use spin-unrestricted (UHF) or spinrestricted open-shell (ROHF) approaches for the HF part and for generating the orbitals for the subsequent single-reference CC calculations. For the latter we used an unrestricted spin-orbital formalism in its singles and doubles variant augmented with a noniterative triples method based on a ROHF reference – the ROHF-CCSD(T) method^{37–40} [also often referred to as 'RHF-UCCSD(T)'].

In order to gauge and understand the problems encountered for the CCSD(T) potential energy surface, we also carried out full CC singles doubles and triples (CCSDT)^{41,42} and CC singles doubles triples augmented with noniterative quadruples [CCSDT(Q)]^{43,44} calculations. For the latter we used the CCSDT(Q)/B variant for ROHF reference.⁴⁵ In addition, we also considered several approximate iterative triples methods including CCSDT-n (n=1b,2,3,4).^{46,47}

The recently published⁴⁸ aug-cc-p(w)CVnZ-PP basis sets for alkali metal and alkaline earth

atoms, designed for the ECP28MDF pseudopotential, have been used (n = 3,4,5), while for all-electron SFX2C-1e based computations, the aug-cc-pwCVTZ-X2C basis set was used.

The ECP-based ROHF-CCSD(T) calculations described above have been performed using the MOL-PRO 2018.2 program package $^{49-53}$, the SFX2C-1e-ROHF-CCSD(T), all CCSD(T) $_{\Lambda}$, $^{54-56}$ CCSDT, and CCSDT-n (n=1b, 2, 3, and 4) calculations have been carried out using the CFOUR program package $^{40,57-59}$, and all CCSDT(Q) energies were computed using the MRCC program suite 44,60,61 .

III. THEORY

Coupled-cluster theory is based on a similarity transformation of the Hamiltonian and a projective solution of the resulting stationary Schrödinger equation. This leads to the equations

$$E = \langle \Phi_0 | \bar{H} | \Phi_0 \rangle \tag{2a}$$

$$0 = \langle \Phi_I | \bar{H} | \Phi_0 \rangle , \qquad (2b)$$

where

$$\bar{H} = e^{-\hat{T}} \hat{H} e^{\hat{T}} \tag{3}$$

is the similarity transformed electronic clampednuclei Hamiltonian and $|\Phi_0\rangle$ the reference wavefunction. The excited determinants $|\Phi_I\rangle$ are chosen to match the excitations reached by he cluster operator $\hat{T} = \sum_n \hat{T}_n$, which consists of *n*-fold excitation operators defined via

$$\hat{T}_n = \frac{1}{(n!)^2} \sum_{ijk,\dots} \sum_{abc,\dots} [T_n]^{abc,\dots}_{ijk,\dots} \hat{a}_a^{\dagger} \hat{a}_b^{\dagger} \hat{a}_c^{\dagger} \cdots \hat{a}_k \hat{a}_j \hat{a}_i \cdots$$

$$\tag{4}$$

Here, the symobls \hat{a}^{\dagger} are creation and the \hat{a} annihilation operators, $[T_n]_{ijk...}^{abc...}$ are the cluster amplitudes and the indices a,b,c,... run over virtual and i,j,k,... over occupied orbitals, respectively. The electronic Hamiltonian \hat{H} is usually formulated as

$$\hat{H} = E_0 + \hat{f}_N + \hat{W}_N \tag{5a}$$

$$= E_0 + \sum_{pq} f_p^q \hat{a}_p^{\dagger} \hat{a}_q + \frac{1}{4} \sum_{pqrs} g_{pr}^{qs} \hat{a}_p^{\dagger} \hat{a}_r^{\dagger} \hat{a}_s \hat{a}_q , \quad (5b)$$

with the one-particle operator \hat{f}_N containing the Fock matrix f_p^q and the two-particle operator \hat{W}_N with the anti-symmetrized two-electron integrals g_{pr}^{qs} . For later reference, we note that the coupled-cluster equations, Eqs. (2), can be summarized as an energy functional⁶²

$$\mathcal{L} = \langle \Phi_0 | (1 + \hat{\Lambda}) \bar{H} | \Phi_0 \rangle \tag{6}$$

where the Lambda operator was introduced, consisting of a set of deexcitation operators with analogous definition to that of the excitation operators of the cluster operator.

For CCSD, the cluster operator is truncated after double excitations, but it is well-known that quantitative computations require at least an approximate account of triple excitations. In order to cut down the computational expense of full CCSDT computations, it is usual to approximate the triple excitations perturbatively. One of the first approaches implemented is the CCSD[T] energy correction [originally called CCSD+T(CCSD)]⁶³, which is based on a fourth-order perturbation theory contribution and is given, assuming canonical (Hartree-Fock) orbitals, in terms of

$$\begin{split} \Delta E^{[T]} &= \Delta E^{(4)} = - \langle \Phi_0 | \hat{T}_3^{\dagger} \hat{f}_N \hat{T}_3 | \Phi_0 \rangle \\ &= -\frac{1}{36} \sum_{ijk} \sum_{abc} \left([T_3]_{ijk}^{abc} \right)^2 \cdot D_{ijk}^{abc} \,, \end{split} \tag{7}$$

with \hat{T}_3 defined via Eq. (4) and D^{abc}_{ijk} expressed in terms of orbital energies ε_p via

$$D_{ijk}^{abc} = \varepsilon_a + \varepsilon_b + \varepsilon_c - \varepsilon_i - \varepsilon_j - \varepsilon_k \tag{8}$$

The triples amplitudes are computed from the converged CCSD amplitudes

$$[T_3]_{ijk}^{abc} = \frac{-\langle \Phi_{ijk}^{abc} | [\hat{W}_N, \hat{T}_{2,\text{CCSD}}] | \Phi_0 \rangle}{\varepsilon_a + \varepsilon_b + \varepsilon_c - \varepsilon_i - \varepsilon_j - \varepsilon_k}, \quad (9)$$

where Φ_{ijk}^{abc} denotes a triply excited determinant. By considering an additional term including CCSD singles excitations one obtains an energy correction, which is formally of fifth-order in the perturbation expansion, yielding

$$\Delta E^{(5)} = \left\langle \Phi_0 \middle| \hat{T}_1^{\dagger} \hat{W}_N \hat{T}_3 \middle| \Phi_0 \right\rangle$$

$$= \frac{1}{4} \sum_{ijk} \sum_{abc} [T_1]_i^a \left\langle bc \middle| jk \right\rangle [T_3]_{ijk}^{abc}. \tag{10}$$

The well-known CCSD(T) method^{37,40} includes this fifth-order term:

$$\Delta E^{(T)} = \Delta E^{(4)} + \Delta E^{(5)} = \Delta E^{[T]} + \Delta E^{(5)}.$$
 (11)

The fifth-order term can be understood in terms of an alternative definition of the unperturbed system⁵⁴ and was shown to be often essential for a good performance of the perturbative triples correction.⁶⁴

In addition, a number of further approximations to CCSDT exist, which treat the triple excitations perturbatively, but include them self-consistently into the solution of the coupled-cluster equations. This is in particular the class of CCSDT-*n* methods of which we in this work consider the variants n =1b, 2, 3, and 4.46,47,65,66 CCSDT-1b can be largely viewed as the self-consistent version of CCSD(T), as it includes the same leading-order terms in the coupled-cluster equations, which also lead to the perturbative energy expression, Eq. (11). In addition, it includes contributions of $\hat{T}_1\hat{T}_3$ to the doubles residual, which is thus complete (compared to the doubles residual of the full CCSDT method). The other methods, CCSDT-2 and CCSDT-3, subsequently include further terms in the residual for the triple excitations, while avoiding any N^8 -scaling contributions. Hence, up to this point the only contribution of the cluster operator \hat{T}_3 in the triple excitation residual appears via $\langle \Phi_{I_3} | \hat{f}_N \hat{T}_3 | \Phi_0 \rangle$ defining an equation for determining the corresponding \hat{T}_3 amplitudes independent of \hat{T}_3 itself. These amplitudes are calculated 'on the fly' immediately followed by calculating the resulting contribution of \hat{T}_3 in the projections onto the singles and doubles subspaces. These computational savings are lost when proceeding to CCSDT-4 which partially includes N^8 terms. This method goes beyond the perturbative approximation of \hat{T}_3 and includes the full term $\langle \Phi_{I_2} | [\hat{H}, \hat{T}_3] | \Phi_0 \rangle$. While the CCSDT-*n* methods do not find wide use for the computation of ground state energies, they provide a useful hierarchy to investigate any short-comings of CCSD(T).

IV. RESULTS

In this work we focus on the calculation of the $X^2\Sigma_g^+$ ground state of Rb_2^+ at ROHF-CCSD(T) level of theory. We note that there is a second state

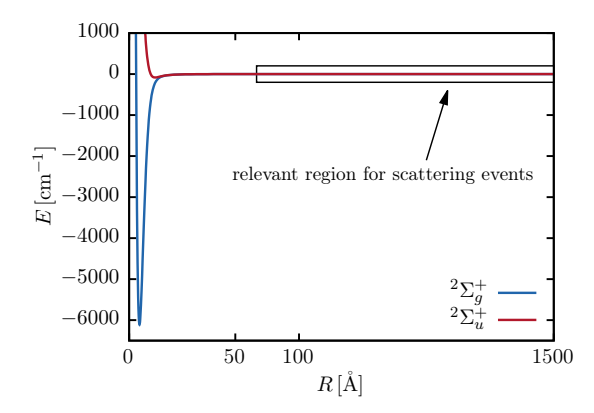


Figure 1. Schematic illustration of complete potential energy curves (PECs) of the $\mathrm{Rb_2}^+$ ground states $^2\Sigma_g^+$ and $^2\Sigma_u^+$. For studying the ion-atom interaction we need high accuracy over the whole range of the PEC to obtain both the rovibrational structure and the long-range region, relevant for investigating scattering events, highly accurate.

of ungerade symmetry (i.e. $(1)^2\Sigma_u^+$) which becomes degenerate to the former one in the long-range region, as shown in Fig. 1.

A. Breakdown of CCSD(T)

In all calculations, we tightened the convergence thresholds for both the underlying ROHF calculations and the subsequent coupled-cluster part as much as possible to avoid numerical errors. Figure 2 gives an overview of the resulting long-range parts of the corresponding PECs for the aug-ccpCVnZ-PP basis sets (n = T, Q, 5). The curves for the ROHF reference and the CCSD energies show the expected long-range behavior, i.e. a weakly attractive potential that decays in accordance with Eq. (1). However, including perturbative triples corrections either via CCSD(T) or CCSD[T] produces a small but clearly unexpected barrier in the long-range region at $R \approx 100 \,\text{Å}$ with a magnitude of $\approx 0.15\,\mathrm{cm}^{-1}$ above the dissociation asymptote. We note that the fifth-order energy correction $\Delta E^{(5)}$ is unproblematic in this respect.

To the best of our knowledge this kind of unphysical behavior seems to be undocumented so far. It appears to be an inherent problem for the CCSD(T)

method, since other sources of error can be excluded after thoroughly investigating their impact (see also supplementary material):

- (i) numerical errors due to convergence issues: We used tightened thresholds a priori, with numerical noise for energies in the order of $< \mathcal{O}(2.5 \cdot 10^{-7} \, \text{cm}^{-1})$.
- (ii) insufficient basis set: As seen in Fig. 2, the shape of the PEC for ROHF-CCSD does not depend on the basis set and the height of the spurious barrier at the ROHF-CCSD(T) level even increases for larger basis sets. This also implies that basis set superposition is not a cause of the problem either, which we could also confirm by applying the counterpoise correction scheme to account for basis set superposition errors.
- (iii) the choice of reference wavefunction: We computed the long-range tail of the PECs using UHF references with the CFOUR program and obtained virtually the same result, with absolute energy differences $\mathcal{O}(10^{-2}\,\mathrm{cm}^{-1})$.
- (iv) use of spin-unrestricted or partially spin-restricted coupled-cluster theory [i.e. RHF-UCCSD(T)] or RHF-RCCSD(T)], see, e.g., Refs. 51–53: This only leads to energy differences in the long-range region in the order of $\mathcal{O}(10^{-4}\,\mathrm{cm}^{-1})$

We also found that this unphysical barrier is universal for X_2^+ systems (X = Li,Na, K, Rb, Cs), which is shown in the supplementary material. The problem further occurs for both the aug-cc-pCVnZ-PP and the aug-cc-pwCVnZ-PP basis set series of Ref. 48 as demonstrated in the supplementary material. Moreover, it is not an artefact due to the approximative nature of the scECP treatment since an all-electron SFX2C-1e-ROHF-CCSD(T) calculation at aug-cc-pwCVTZ-X2C level of theory leads to the long-range behavior shown in Fig. 3. Obviously, the long-range barrier is still present, at the same position with the same order of magnitude. Finally, we note that there are no multireference effects expected for the Rb₂⁺ system. The two near-degenerate states $(X^2\Sigma_g^+ \text{ and } (1)^2\Sigma_u^+)$ are of different symmetry and thus do not mix. This

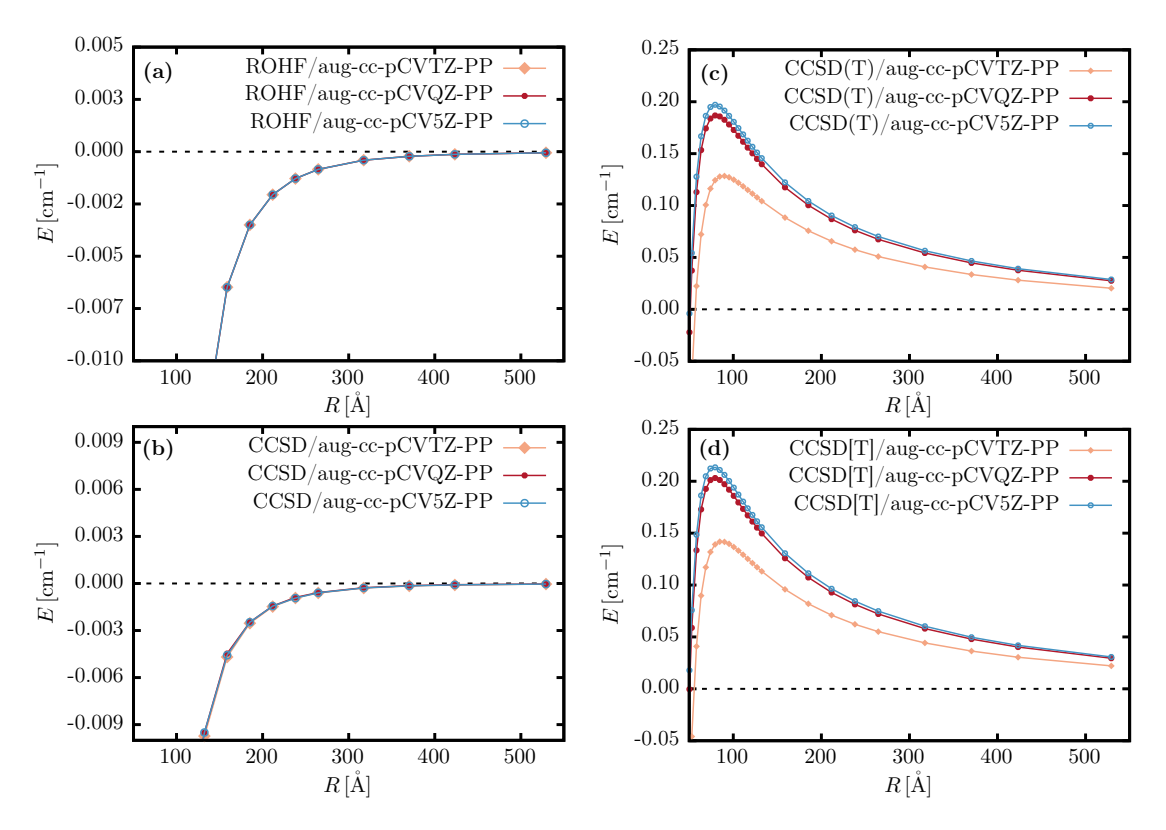


Figure 2. Overview of the long-range parts of the PECs of the Rb₂⁺ ground state calculated at different levels of theory each using ECP28MDF. In (a) the reference energies (ROHF) are shown for the aug-cc-pCVnZ-PP basis sets. In (b) the coupled-cluster energies with single and double excitations (CCSD) are shown. From Figs. (c) and (d) we obtain that including perturbative triples in the coupled-cluster method either via (T) or [T] lead to unphysical humps in the long-range region. All energies are given as interaction energies relative to the asymptote.

is in contrast to what has been reported, e.g., in Ref. 67 for the ground state PEC of neutral LiNa, where indeed multireference effects are present and CCSD(T) fails to correctly describe the bond cleavage.

B. Higher excitations and iterative approximations

CCSD[T] and CCSD(T) are non-iterative approximations to CCSDT. To further investigate the origin of the long-range hump we also applied iterative approximations to full CCSDT: the CCSDT-n, with n = 1b, 2, 3, 4, methods^{46,47,65}. We used the ECP28MDF pseudopotential and the aug-cc-pCVTZ-PP basis set in these calculations.

As outlined in Sec. III these methods include contributions due to triples excitations conveyed via \hat{T}_3 into the solution of the coupled-cluster equations. Here all approaches, except the CCSDT-4 method, avoid including any terms with N^8 scaling.

The resulting long-range PECs of these iterative approximations to CCSDT are shown in Fig. 4 (a). Again, we obtain a hump for CCSDT-1b, CCSDT-2, CCSDT-3 at the same position ($\approx 100\,\text{Å}$) and of the same magnitude ($\approx 0.1\,\text{cm}^{-1}$) as we have already seen for the non-iterative methods. Including more terms in the approximation scheme leads to a decrease in the size of the barrier. However, only with the inclusion of the full Hamiltonian in the projection onto the excited triples manifold, i.e. for CCSDT-4, the artificial barrier disappears. But, as

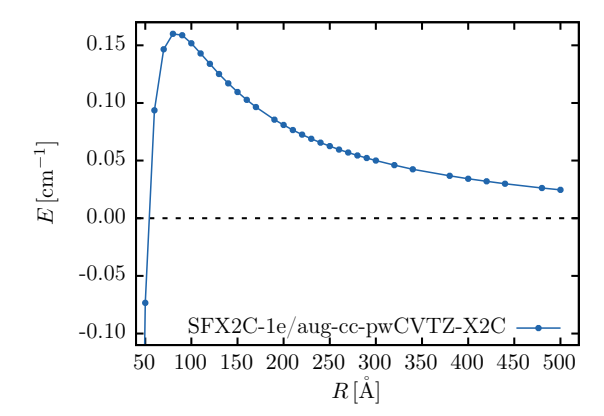


Figure 3. All-electron SFX2C-1e calculation at ROHF-CCSD(T)/aug-cc-pwCVTZ-X2C level of theory. The energies are given as interaction energies relative to the asymptote.

already mentioned this method is already as expensive as the full CCSDT calculation. The resulting long-range tails are presented in Fig. 4 (b) with both methods leading to the same shape in the asymptotic region.

This suggests the hypothesis that the $\langle \Phi_0 | \hat{T}_3^\dagger \hat{f}_N \hat{T}_3 | \Phi_0 \rangle$ term, shared by all problematic methods (CCSD[T]/CCSD(T) as well), does not correctly account for interatomic interactions. In fact, this term only contains the interaction with the Hartree-Fock density of the other atom.

We obtain the same phenomenon if we perturbatively include even higher excitations such as CCSDT(Q). The corresponding result is shown in Fig. 4 (c). The hump is smaller in size, as the contributions of connected quadruples are generally smaller than those of connected triples. Nevertheless, despite its smallness the artificial barrier completely spoils the long-range behavior of the potential, which is important for correct predictions of the scattering physics.

C. Symmetry breaking

In general X_2^+ – systems, with X = Li, Na, K, Rb, Cs, are characterized by the point group $D_{\infty h}$. This implies the asymptotical indistinguishability of Rb⁺+Rb and Rb+Rb⁺, which is also clear from

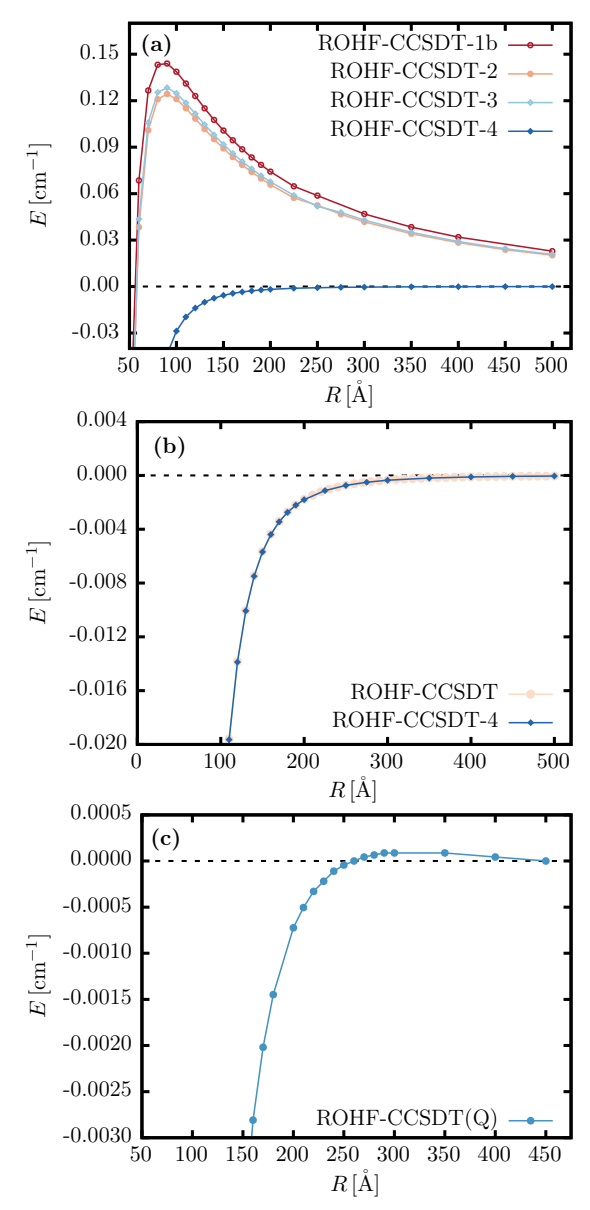


Figure 4. (a) Long-range part of the interaction energies using different iterative approximations to CCSDT. (b) Comparison of CCSDT-4 and full CCSDT interaction energies. Computatations are based on the ECP28MDF pseudopotential, the aug-cc-pCVTZ-PP basis set and a ROHF reference. (c) ROHF-CCSDT(Q) long-range tail of the respective PEC calculated with the MRCC program suite using ECP28MDF/aug-cc-pwCVTZ-PP. The energies in (a) and (b) are given relative to the asymptote while in (c) they are given w.r.t. the last *ab-initio* point.

a fundamental quantum mechanical point of view. The correct asymptotic behavior is given in terms of a superposition of both limiting cases, i.e.

$$|X^{2}\Sigma_{g}^{+}\rangle = \frac{1}{\sqrt{2}}(|0,+\rangle + |+,0\rangle)$$
 (12a)

$$|(1)^{2}\Sigma_{u}^{+}\rangle = \frac{1}{\sqrt{2}}(|0,+\rangle - |+,0\rangle).$$
 (12b)

The zeroth-order description of the system is a mean-field approximation (Hartee-Fock), which involves the self-consistent-field (SCF) solution for the corresponding equations. This need for selfconsistent solutions leads to different orbitals for Rb⁺ and Rb and with that the solution of the separated fragments is in conflict with the symmetry requirement that the two cases Rb⁺+Rb and vice versa are quantum-mechanically indistinguishable. All the orbitals of Rb and Rb⁺ are a "compromise" of the neutral and ionic orbitals. The mean-field solution also defines the Fockian, the effective oneelectron potential of the system and plays an important role for defining perturbative approximations in the coupled-cluster equations. Rather than describing the correct superposition, it contains the compromise solution with half an electron on the right and half an electron on the left side, possibly explaining the repulsive long-range barrier as a consequence of a leading-order repulsive 1/R component in the respective interaction potentials.

If this is true, breaking the symmetry of the system to $C_{\infty\nu}$ should lead to a correct asymptotic behavior without any barrier. Quantum mechanically speaking we project on one of the two limiting cases $(|0,+\rangle = \text{Rb} + \text{Rb}^+$ or vice versa $|+,0\rangle$). To test this hyothesis, we carried out CCSD and CCSD(T) computations using symmetry-broken ROHF orbitals. The resulting long-range tails of the PECs are given in Fig. 5.

The results demonstrate that the long-range hump can indeed be avoided by reducing the symmetry to $C_{\infty\nu}$. At short-range these symmetry-broken solutions collapse to the symmetric one. This is illustrated in more detail in the supplementary material. Furthermore, the doubly logarithmic analysis in Fig. 5 (d) clearly reveals a repulsive 1/R component in the long-range tail of the symmetry-adapted CCSD(T) PEC. In contrast, the symmetry-broken

solution results in a curve with the correct R^{-4} behavior

The findings suggest that the best model for the long-range region is based on the symmetry-broken solutions. So far the most promising approach is to use symmetry-broken (T) and (Q) corrections for the long-range tail and properly merge with symmetry-adapted solutions for smaller internuclear distances. With this all terms of the outlined additivity scheme according to Sec. II are well-defined paving the way for a highly accurate PEC. The details on this will be published in a subsequent study.

Beyond that, we tested alternative approaches such as the electron affinity equation-of-motion coupled-cluster (EA-EOM-CC) method in the spirit of the approaches on Li2+, Na2+ and K2+ reported in Refs. 21-23. Preliminary results at EA-EOM-CCSD level of theory⁶⁸ using CFOUR look quite promising with similiar performance to CCSD. These findings are reported in the supplementary material. We further examined the applicability of completely renormalized CC (CR-CC) methods such as the CR-CC(2,3),A and CR-CC(2,3),D variants, cf. Refs. 69-72, where corresponding calculations were performed using the GAMESS program package. 73,74 We observed that CR-CC(2,3),A leads to the same long-range barrier as obtained for CCSD(T) with a leading-order repulsive 1/R component. At variance, the CR-CC(2,3),D variant does not feature a repulsive barrier, but instead - somewhat surprisingly - an attractive 1/R component, which also leads to a wrong asymptotic behavior. This is discussed in more detail in the supplementary material.

V. DISCUSSION

Our findings so far suggest that the physical origin of the artificial long-range humps is connected with the underlying mean-field character of our calculations and the way it enters perturbative coupled-cluster approximations. However, it is not clear if this problem is caused by the approximation in the energy expression or due to the use of approximate triples amplitudes. The latter can be tested rather systematically by using \hat{T}_3 amplitudes from CCSDT

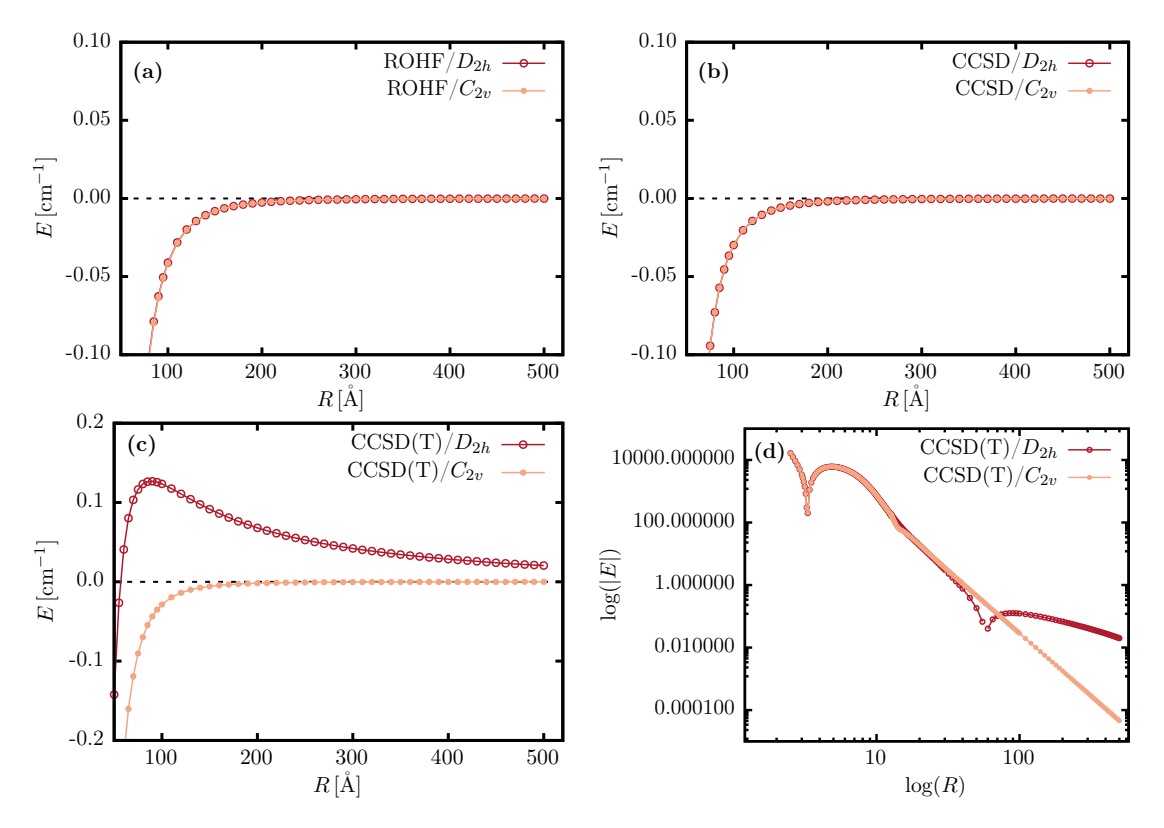


Figure 5. Comparison of the long-range parts using either symmetry-adapted (D_{2h}) or symmetry-broken $(C_{2\nu})$ ROHF orbitals. In (a) the reference (ROHF) interaction energies are shown. In (b) the CCSD results are depicted, while (c) shows the CCSD(T) interaction energies. (d) Comparison of the symmetry-adapted and symmetry-broken CCSD(T) PECs in doubly logarithmic representation. The long-range tail of the symmetry-adapted CCSD(T) curve clearly exhibits a repulsive 1/R component resulting from the problems related with the mean-field approach (see text). The tiny deviation of the symmetry-broken solution for $\approx 12 - 20 \text{Å}$ is due to a numerical bistability discussed in more detail in the supporting information. All energies are given as interaction energies relative to the asymptote.

in Eq. (7).

We first carried out calculations using a closely related formulation for the triples contribution based on analytic energy derivative formulation of CCSD. 75,76 A CCSD Lagrangian 62,77 with triple excitations treated as an "external" perturbation with a fictitious field strength χ is used here

$$\mathcal{L}(\hat{T}_1, \hat{T}_2, \chi \hat{T}_3) = \langle 0 | (1 + \hat{\Lambda}_{CCSD}) \bar{H}[\chi] | 0 \rangle, \quad (13)$$

in which $\hat{\Lambda}_{\text{CCSD}} = \hat{\Lambda}_{1,\text{CCSD}} + \hat{\Lambda}_{2,\text{CCSD}}$ represents the CCSD Λ operator, and \hat{T}_3 contributes to \bar{H} , defined in Eq. (3), in the same way as in the CCSDT method. Given the exact \hat{T}_3 , a finite-field CCSD calculation

defined as the left-hand side of Eq. (13) with $\chi=1$ produces the exact CCSDT energy. This finite field CCSD calculation uses the CCSDT equation, but treats the triples as the perturbation. Hence the

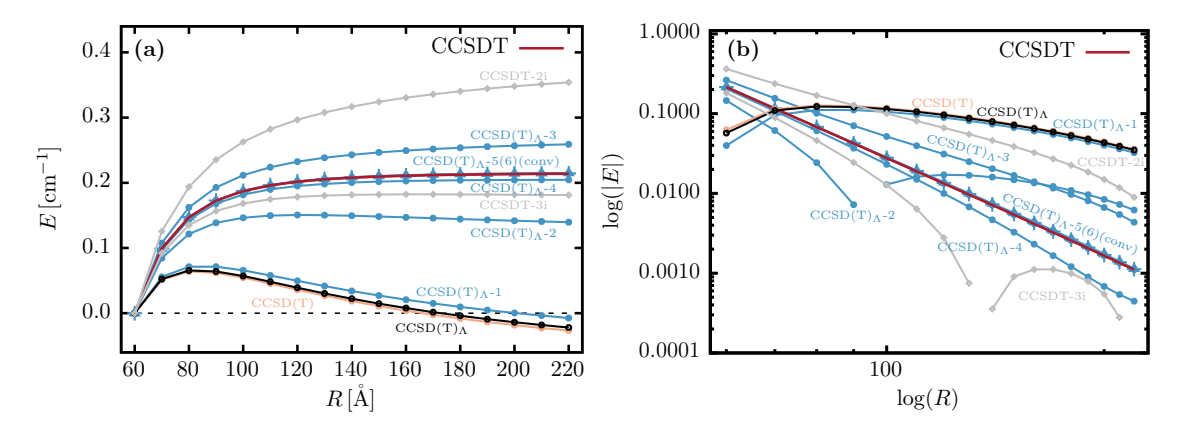


Figure 6. (a) Comparison of potential energy curves of Rb_2^+ calculated with ECP28MDF/aug-cc-pwCVTZ-PP and different levels of the $CCSD(T)_{\Lambda}$ -n method introduced in this work (see text for more details). The method refers to the use of \hat{T}_3 amplitudes obtained at the n'th CCSDT iteration. $CCSD(T)_{\Lambda}$ -conv denotes the use of converged triples amplitudes. CCSDT-2i(3i) is the CCSDT energy after the second (third) iteration. All PECs are plotted w.r.t. $R = 60 \,\text{Å}$. (b) Doubly logarithmic representation of the curves from panel (a) with respect to the extrapolated limit for $R \to \infty$.

CCSDT energy can be expanded in a Taylor series

$$\begin{split} E_{\text{CCSDT}} &= \mathcal{L}(\hat{T}_1, \hat{T}_2, \chi \hat{T}_3) \Big|_{\chi=1} \\ &= \left[\mathcal{L} \Big|_{\chi=0} + \chi \frac{\mathrm{d}\mathcal{L}}{\mathrm{d}\chi} \Big|_{\chi=0} \right. \\ &+ \frac{1}{2} \chi^2 \frac{\mathrm{d}^2 \mathcal{L}}{\mathrm{d}\chi^2} \Big|_{\chi=0} + \cdots \Big]_{\left. \chi=1 \right.} \\ &= \mathcal{L} \Big|_{\chi=0} + \frac{\mathrm{d}\mathcal{L}}{\mathrm{d}\chi} \Big|_{\chi=0} + \frac{1}{2} \frac{\mathrm{d}^2 \mathcal{L}}{\mathrm{d}\chi^2} \Big|_{\chi=0} + \cdots, \end{split}$$

with the unperturbed energy being the CCSD energy

$$\mathscr{L}\Big|_{\gamma=0} = E_{\text{CCSD}} \tag{15}$$

and the first-order correction given by

$$\frac{\mathrm{d}\mathscr{L}}{\mathrm{d}\chi}\Big|_{\chi=0} = \left\langle 0 \left| \hat{\Lambda}_{\text{CCSD}} \frac{\partial \bar{H}[\chi]}{\partial \chi} \right| 0 \right\rangle_{\chi=0}$$

$$= \left\langle 0 \left| \hat{\Lambda}_{\text{CCSD}}[\hat{H}, \hat{T}_3] \right| 0 \right\rangle. \tag{16}$$

Eq. (16) offers a flexible framework for obtaining leading triples corrections to the CCSD energy. When the leading-order contribution to \hat{T}_3 is used, i.e. the triples amplitudes defined in Eq. (9),

Eq. (16) reduces to the CCSD(T) $_{\Lambda}$ method originally derived within the equation-of-motion CC framework.⁵⁴⁻⁵⁶ Eq. (16) is also compatible with the use of improved \hat{T}_3 amplitudes obtained from iterative solutions of the CCSDT amplitude equations. This is particularly useful for the present purpose to understand whether the small humps in the CCSD(T) potential energy curves originate from the approximation in the energy expression or from the approximation of using the approximate \hat{T}_3 as in Eq. (9). A straightforward approach to improve \hat{T}_3 is to solve the CCSDT amplitude equations iteratively. Here we define $E_T[CCSD(T)_{\Lambda}$ -n] as the triples energy correction using Eq. (16) with $\hat{T}_{3,n'th}$ obtained from the n'th iteration of CCSDT equations with converged CCSD amplitudes adopted as the initial guess

$$E_{\rm T}[{\rm CCSD}({\rm T})_{\Lambda}-{\rm n}] = \langle 0|\hat{\Lambda}_{\rm CCSD}[\hat{H},\hat{T}_{3,{\rm n}'{\rm th}}]|0\rangle$$
. (17)

The use of T_3 from a converged CCSDT calculation provides the first-order correction from the triples amplitudes to the CCSD energy

$$E_{\rm T}[{\rm CCSD}({\rm T})_{\Lambda}{\rm -conv}] = \langle 0|\hat{\Lambda}_{\rm CCSD}[\hat{H},\hat{T}_{3,{\rm CCSDT}}]|0\rangle$$
. (18)

Here "-conv" denotes the use of converged CCSDT \hat{T}_3 . Although it is obviously not practically useful,

Eq. (18) defines the limit of the accuracy that can be obtained using Eq. (16).

The CCSD(T) $_{\Lambda}$ -n methods are related to available methods for obtaining triples corrections, ^{78–84} the most intimately to the CCSD(T-n) methods⁸²⁻⁸⁴ derived using CCSD Lagrangian, which also treats CCSD as the unperturbed state. The difference lies in that the schemes outlined so far refrain from performing an Møller-Plesset perturbation analysis and limit the consideration to the first derivative with respect to the triples amplitudes, whereas, the CCSD(T-n) derivation expands the Lagrangian order by order in terms of the fluctuation potential. Since the first iteration of the CCSDT amplitude equations in $CCSD(T)_{\Lambda}$ -n uses CCSD solutions as the initial guess and generates first-order \hat{T}_3 , substituting this \hat{T}_3 into Eq. (16) gives a triples correction correct to second-order, i.e., $CCSD(T)_{\Lambda}$ -1 is identical to CCSD(T-2). CCSD(T-4) contains contributions from higher orders, i.e., the second term in Eq. (14), which is not considered in CCSD(T) $_{\Lambda}$ -n. The CCSD(T-n) methods are more efficient, since no storage of T_3 is needed. However, the CCSD(T) $_{\Lambda}$ n approaches may have the advantage that the use of convergence-acceleration techniques during iterative solutions of CCSDT equation such as direct inverse of iterative space (DIIS)⁸⁵ may smooth the convergence when the plain iterative solutions exhibit an oscillating behavior.

We have performed CCSD(T)_{Λ}-n,n = 1 - 6 and $CCSD(T)_{\Lambda}$ - ∞ calculations for potential energy surfaces of Rb₂⁺ using the aug-cc-pwCVTZ-PP basis set. As shown in Fig. 6 (a), the CCSD(T) $_{\Lambda}$ -n results systematically converge to the $CCSD(T)_{\Lambda}$ - ∞ results, which is essentially indistinguishable from CCSDT results. The CCSD(T) $_{\Lambda}$ -1 curve shows an artificial hump similar to the case of $CCSD(T)_{\Lambda}$. The hump is significantly reduced in the CCSD(T) $_{\Lambda}$ -2 curve and is eliminated using methods with more than two iterations. The doubly logarithmic representation in Fig. 6 (b) shows, however, that the recovery of the correct long-range behavior proceeds more slowly. CCSD(T)_{Λ}-3 still is dominated by an R^{-3} component in the range plotted in the figure, while $CCSD(T)_{\Lambda}$ -4 decays too quickly in this range, showing an R^{-5} behavior. From order 5 on, the method has essentially converged to the correct R^{-4} behavior. These results clearly support that the artificial

hump in the CCSD(T) curve and the wrong asymptotic behavior originates from the approximation of \hat{T}_3 . This is also true for iterative approximations to CCSDT, i.e. CCSDT-n (n = 1b, 2, 3) since the equation for the approximate triples amplitudes is formally similar to Eq. (9).

Note that the CCSD(T)_{Λ}-n energies converge more rapidly than CCSDT energies with respect to iterative solution of CCSDT amplitude equations, as also demonstrated in Fig. 6. The CCSDT-2i energies lead to a PEC with a leading-order attractive R^{-3} component similar to CCSD(T)_{Λ}-3, while the CCSDT-3i results also reveal a tiny repulsive barrier, see Fig. 6 (b). The CCSD(T)_{Λ}-n triples correction is less sensitive to the quality of \hat{T}_3 , since it is only a small fraction of the total CCSDT energy. Finally, we note that, while the CCSD(T)_{Λ}-n methods have proven useful in the present context, the potential usefulness in calculations of chemical properties remains to be explored.

VI. CONCLUSION

This work shows that several standard coupledcluster methods with noniterative or approximative iterative treatments of triple excitations can lead to unphysical potential energy curves for X₂⁺ systems, $X \in \{Li, Na, K, Rb, Cs\}$, with a spurious longrange repulsive 1/R component leading to a barrier at around 100 Å (for the case of Rb₂⁺). Although this effect is in the order $\mathcal{O}(10^{-1}\,\mathrm{cm}^{-1})$ it would lead to severe problems when using the corresponding PECs for highly accurate studies in the context of ultracold chemistry. We unraveled the origin of this phenomenon by studying the ground state PEC of Rb₂⁺. It arises from the need to define self-consistent solutions which at the same time cannot be both consistent with the separated fragments (different orbitals for Rb+ and Rb) and with the quantum mechanically imposed symmetry requirement (indistinguishable cases Rb⁺+Rb and Rb+Rb⁺). The resulting asymptotic orbitals thus correspond to two +0.5-fold charged ions. This problem lives on in the Fockian and affects the perturbative estimates of the \hat{T}_3 amplitudes, which finally lead to the wrong behavior of the PEC. This was demonstrated quantitatively by using a new

"CCSD(T) $_{\Lambda}$ -n" scheme.

For the Rb2⁺ molecule we found that symmetry-broken CCSD(T) solutions lead to physically correct long-range PECs while symmetry-broken and non-broken CCSD curves virtually coincide in this region. From this we conclude that (T) corrections from symmetry- broken calculations can be used for estimating the complete basis set limit of the long-range part of the PEC. In the same way we could proceed with (Q) corrections and smaller basis sets eventually defining a protocol for obtaining a highly accurate global PEC for the ground state of Rb2⁺. This will be thoroughly investigated in a subsequent study.

SUPPLEMENTARY MATERIAL

See supplementary material for technical details on the independence of the long-range hump on possible sources of error and different basis sets, for the universality of the current problem for X_2^+ systems and for more details on symmetry breaking and tests for alternative coupled-cluster methods.

ACKNOWLEDGMENTS

J.S. and A.K. would like to acknowledge funding by IQST. The research of IQST is financially supported by the Ministry of Science, Research, and Arts Baden-Württemberg. Furthermore, the authors acknowledge support by the state of Baden-Württemberg through bwHPC and the German Research Foundation (DFG) through grant no INST 40/575-1 FUGG (JUSTUS 2 cluster). The work at Johns Hopkins university has been supported by the National Science Foundation, under grant No. PHY-2011794.

DATA AVAILABILITY

The data that support the findings of this study are available within this article and its supplementary material.

REFERENCES

¹W. Ketterle, Rev. Mod. Phys. **74**, 1131 (2002).

²M. Schlagmüller, T. C. Liebisch, F. Engel, K. S. Kleinbach, F. Böttcher, U. Hermann, K. M. Westphal, A. Gaj, R. Löw, S. Hofferberth, T. Pfau, J. Pérez-Ríos, and C. H. Greene, Phys. Rev. X 6, 031020 (2016).

³T. C. Liebisch, M. Schlagmüller, F. Engel, H. Nguyen, J. Balewski, G. Lochead, F. Böttcher, K. M. Westphal, K. S. Kleinbach, T. Schmid, A. Gaj, R. Löw, S. Hofferberth, T. Pfau, J. Pérez-Ríos, and C. H. Greene, J. Phys. B 49, 182001 (2016).

⁴F. Böttcher, A. Gaj, K. M. Westphal, M. Schlagmüller, K. S. Kleinbach, R. Löw, T. C. Liebisch, T. Pfau, and S. Hofferberth, Phys. Rev. A **93**, 032512 (2016).

⁵M. Deiß, B. Drews, J. Hecker Denschlag, N. Bouloufa-Maafa, R. Vexiau, and O. Dulieu, New J. Phys. 17, 065019 (2015).

⁶B. Drews, M. Deiß, K. Jachymski, Z. Idziaszek, and J. Hecker Denschlag, Nature Commun. **8**, 14854 (2017).

⁷B. Drews, M. Deiß, J. Wolf, E. Tiemann, and J. Hecker Denschlag, Phys. Rev. A **95**, 062507 (2017).

⁸M. Tomza, K. Jachymski, R. Gerritsma, A. Negretti, T. Calarco, Z. Idziaszek, and P. S. Julienne, Rev. Mod. Phys. 91, 035001 (2019).

⁹R. Côté and A. Dalgarno, Phys. Rev. A **62**, 012709 (2000).

¹⁰Z. Idziaszek, T. Calarco, P. S. Julienne, and A. Simoni, Phys. Rev. A **79**, 010702 (2009).

¹¹T. Schmid, C. Veit, N. Zuber, R. Löw, T. Pfau, M. Tarana, and M. Tomza, Phys. Rev. Lett. **120**, 153401 (2018).

¹²K. Kleinbach, F. Engel, T. Dieterle, R. Löw, T. Pfau, and F. Meinert, Phys. Rev. Lett. **120**, 193401 (2018).

¹³F. Engel, T. Dieterle, T. Schmid, C. Tomschitz, C. Veit, N. Zuber, R. Löw, T. Pfau, and F. Meinert, Phys. Rev. Lett. **121**, 193401 (2018).

¹⁴S. H. Patil and K. T. Tang, J. Chem. Phys. **106**, 2298 (1997).

¹⁵K. Jachymski, M. Krych, P. S. Julienne, and Z. Idziaszek, Phys. Rev. Lett. **110**, 213202 (2013).

¹⁶K. Jachymski, M. Krych, P. S. Julienne, and Z. Idziaszek, Phys. Rev. A **90**, 042705 (2014).

¹⁷S. Magnier, S. Rousseau, A. Allouche, G. Hadinger, and M. Aubert-Frécon, Chem. Phys. **246**, 57 (1999).

¹⁸H. Berriche, Int. J. Quant. Chem. **113**, 2405 (2013).

¹⁹S. Magnier and M. Aubert-Frécon, J. Quant. Spectrosc. Ra. 78, 217 (2003).

²⁰A. Jraij, A. Allouche, M. Korek, and M. Aubert-Frécon, Chem. Phys. **290**, 129 (2003).

²¹M. Musiał, M. Medrek, and S. A. Kucharski, Mol. Phys. **113**, 2943 (2015).

²²A. Bewicz, M. Musiał, and S. A. Kucharski, Mol. Phys. **115**, 2649 (2017).

²³P. Skupin, M. Musiał, and S. A. Kucharski, J. Phys. Chem. A **121**, 1480 (2017).

²⁴S. H. Yuwono, I. Magoulas, and P. Piecuch, Sci. Adv. 6 (2020), 10.1126/sciadv.aay4058.

²⁵I. Magoulas, N. P. Bauman, J. Shen, and P. Piecuch, J. Phys. Chem. A **122**, 1350 (2018).

²⁶D. Feller, J. Chem. Phys. **98**, 7059 (1993).

- ²⁷T. Helgaker, W. Klopper, H. Koch, and J. Noga, J. Chem. Phys. **106**, 9639 (1997).
- ²⁸J. M. L. Martin and G. de Oliveira, J. Chem. Phys. **111**, 1843 (1999).
- ²⁹ A. Tajti, P. G. Szalay, A. G. Császár, M. Kállay, J. Gauss, E. F. Valeev, B. A. Flowers, J. Vázquez, and J. F. Stanton, J. Chem. Phys. **121**, 11599 (2004).
- ³⁰M. S. Schuurman, S. R. Muir, W. D. Allen, and H. F. Schaefer III, J. Chem. Phys. **120**, 11586 (2004).
- ³¹D. Feller, K. A. Peterson, and D. A. Dixon, J. Chem. Phys. **129**, 204105 (2008).
- ³²J. J. Eriksen, D. A. Matthews, P. Jørgensen, and J. Gauss, J. Chem. Phys. **144**, 194102 (2016).
- ³³J. J. Eriksen, D. A. Matthews, P. Jørgensen, and J. Gauss, J. Chem. Phys. **144**, 194103 (2016).
- ³⁴I. S. Lim, P. Schwerdtfeger, B. Metz, and H. Stoll, J. Chem. Phys. **122**, 104103 (2005).
- ³⁵K. G. Dyall, J. Chem. Phys. **115**, 9136 (2001).
- ³⁶W. Liu and D. Peng, J. Chem. Phys. **131**, 1 (2009).
- ³⁷K. Raghavachari, G. W. Trucks, J. A. Pople, and M. Head-Gordon, Chem. Phys. Lett. **157**, 479 (1989).
- ³⁸R. J. Bartlett, J. D. Watts, S. A. Kucharski, and J. Noga, Chem. Phys. Lett. **165**, 513 (1990).
- ³⁹C. Hampel, K. A. Peterson, and H.-J. Werner, Chem. Phys. Lett. **190**, 1 (1992).
- ⁴⁰J. D. Watts, J. Gauss, and R. J. Bartlett, Chem. Phys. Lett. **200**, 1 (1992).
- ⁴¹ J. Noga and R. J. Bartlett, J. Chem. Phys. **86**, 7041 (1987).
- ⁴²G. E. Scuseria and H. F. Schaefer III. Chem. Phys. Lett. **152**, 382 (1988).
- ⁴³Y. J. Bomble, J. F. Stanton, M. Kállay, and J. Gauss, J. Chem. Phys. **123**, 054101 (2005).
- ⁴⁴M. Kállay and J. Gauss, J. Chem. Phys. **123**, 214105 (2005).
- 45 M. Kállay and J. Gauss, J. Chem. Phys. **129**, 144101 (2008).
- ⁴⁶Y. S. Lee, S. A. Kucharski, and R. J. Bartlett, J. Chem. Phys. **81**, 5906 (1984).
- ⁴⁷J. Noga, R. J. Bartlett, and M. Urban, Chem. Phys. Lett. **134**, 126 (1987).
- ⁴⁸J. G. Hill and K. A. Peterson, J. Chem. Phys. **147**, 244106 (2017).
- ⁴⁹H.-J. Werner, P. J. Knowles, G. Knizia, F. R. Manby, and M. Schütz, WIREs Comput. Mol. Sci. 2, 242 (2012).
- ⁵⁰H.-J. Werner, P. J. Knowles, G. Knizia, F. R. Manby, M. Schütz, et al., "Molpro, version 2018.2, a package of ab initio programs," (2018), see http://www.molpro.net.
- ⁵¹P. J. Knowles, C. Hampel, and H. J. Werner, J. Chem. Phys. **99**, 5219 (1993).
- ⁵²P. J. Knowles, C. Hampel, and H.-J. Werner, J. Chem. Phys. **112**, 3106 (2000).
- ⁵³J. D. Watts, J. Gauss, and R. J. Bartlett, J. Chem. Phys. **98**, 8718 (1993).
- ⁵⁴J. F. Stanton, Chem. Phys. Lett. **281**, 130 (1997).
- 55T. D. Crawford and J. F. Stanton, Int. J. Quantum Chem. **70**, 601 (1998).
- ⁵⁶S. A. Kucharski and R. J. Bartlett, J. Chem. Phys. **108**, 5243 (1998).
- ⁵⁷J. F. Stanton, J. Gauss, L. Cheng, M. E. Harding, D. A. Matthews, and P. G. Szalay, "CFOUR, Coupled-Cluster tech-

- niques for Computational Chemistry, a quantum-chemical program package," With contributions from A.A. Auer, R.J. Bartlett, U. Benedikt, C. Berger, D.E. Bernholdt, S. Blaschke, Y. J. Bomble, S. Burger, O. Christiansen, D. Datta, F. Engel, R. Faber, J. Greiner, M. Heckert, O. Heun, M. Hilgenberg, C. Huber, T.-C. Jagau, D. Jonsson, J. Jusélius, T. Kirsch, K. Klein, G.M. KopperW.J. Lauderdale, F. Lipparini, T. Metzroth, L.A. Mück, D.P. O'Neill, T. Nottoli, D.R. Price, E. Prochnow, C. Puzzarini, K. Ruud, F. Schiffmann, W. Schwalbach, C. Simmons, S. Stopkowicz, A. Tajti, J. Vázquez, F. Wang, J.D. Watts and the integral packages MOLECULE (J. Almlöf and P.R. Taylor), PROPS (P.R. Taylor), ABACUS (T. Helgaker, H.J. Aa. Jensen, P. Jørgensen, and J. Olsen), and ECP routines by A. V. Mitin and C. van Wüllen. For the current version, see http://www.cfour.de.
- ⁵⁸D. A. Matthews, L. Cheng, M. E. Harding, F. Lipparini, S. Stopkowicz, T.-C. Jagau, P. G. Szalay, J. Gauss, and J. F. Stanton, J. Chem. Phys. **152**, 214108 (2020).
- ⁵⁹L. Cheng and J. Gauss, J. Chem. Phys. **135**, 084114 (2011).
- ⁶⁰M. Kállay, P. R. Nagy, Z. Rolik, D. Mester, G. S. J. Csontos, J. Csóka, B. P. Szabó, L. Gyevi-Nagy, I. Ladjánszki, L. Szegedy, B. Ladóczki, K. Petrov, M. Farkas, P. D. Mezei, and B. Hégely, "MRCC, a quantum chemical program suite," (2019), see www.mrcc.hu.
- ⁶¹M. Kállay and P. R. Surján, J. Chem. Phys. **115**, 2945 (2001).
- ⁶²J. Arponen, Ann. Phys. **151**, 311 (1983).
- ⁶³M. Urban, J. Noga, S. J. Cole, and R. J. Bartlett, J. Chem. Phys. **83**, 4041 (1985).
- ⁶⁴J. F. Stanton, W. N. Lipscomb, D. H. Magers, and R. J. Bartlett, J. Chem. Phys. **90**, 1077–1082 (1989).
- ⁶⁵Y. He, Z. He, and D. Cremer, Theor. Chem. Acc. **105**, 182 (2001).
- ⁶⁶M. Urban, I. Cernusak, V. Kellö, and J. Noga, *Electron correlation in atoms and molecules*. *Methods in computational chemistry*, Vol. 1 (S. Wilson (ed), New York, 1987) p. 117.
- ⁶⁷D. A. Fedorov, A. Derevianko, and S. A. Varganov, J. Chem. Phys. **140**, 184315 (2014).
- ⁶⁸M. Nooijen and R. J. Bartlett, J. Chem. Phys. **102**, 3629 (1995).
- ⁶⁹P. Piecuch and M. Włoch, J. Chem. Phys. **123**, 224105 (2005).
 ⁷⁰P. Piecuch, M. Włoch, J. R. Gour, and A. Kinal,
- Chem. Phys. Lett. 418, 467 (2006).
 M. Włoch, M. D. Lodriguito, P. Piecuch, and J. R. Gour, Mol. Phys. 104, 2149 (2006).
- ⁷²M. Włoch, J. R. Gour, and P. Piecuch, J. Phys. Chem. A **111**, 11359 (2007).
- ⁷³M. W. Schmidt, K. K. Baldridge, J. A. Boatz, S. T. Elbert, M. S. Gordon, J. H. Jensen, S. Koseki, N. Matsunaga, K. A. Nguyen, S. Su, T. L. Windus, M. Dupuis, and J. A. Montgomery Jr, J. Comput. Chem. 14, 1347 (1993).
- ⁷⁴G. M. J. Barca, C. Bertoni, L. Carrington, D. Datta, N. De Silva, J. E. Deustua, D. G. Fedorov, J. R. Gour, A. O. Gunina, E. Guidez, T. Harville, S. Irle, J. Ivanic, K. Kowalski, S. S. Leang, H. Li, W. Li, J. J. Lutz, I. Magoulas, J. Mato, V. Mironov, H. Nakata, B. Q. Pham, P. Piecuch, D. Poole, S. R. Pruitt, A. P. Rendell, L. B. Roskop, K. Ruedenberg, T. Sattasathuchana, M. W. Schmidt, J. Shen, L. Slipchenko, M. Sosonkina, V. Sundriyal, A. Tiwari, J. L. Galvez Vallejo,

- B. Westheimer, M. Włoch, P. Xu, F. Zahariev, and M. S. Gordon, J. Chem. Phys. **152**, 154102 (2020).
- ⁷⁵L. Adamowicz and R. J. Bartlett, Int. J. Quantum Chem. Symp. 26, 245 (1984).
- ⁷⁶A. C. Scheiner, G. E. Scuseria, J. E. Rice, T. J. Lee, and H. F. Schaefer III, J. Chem. Phys. **87**, 5361 (1987).
- ⁷⁷T. Helgaker and P. Jørgensen, Adv. Quant. Chem. **19**, 188 (1988).
- ⁷⁸S. Hirata, M. Nooijen, I. Grabowski, and R. J. Bartlett, J. Chem. Phys. **114**, 3919 (2001).
- ⁷⁹M. W. Włoch and P. Piecuch, J. Chem. Phys. **123**, 224105 (2005).
- ⁸⁰M. W. Włoch, M. D. Lodriguito, P. Piecuch, and J. R. Gour, Mol. Phys. **104**, 2149 (2006).
- ⁸¹M. W. Włoch, M. D. Lodriguito, P. Piecuch, and J. R. Gour, Mol. Phys. **104**, 2991 (2006).
- ⁸²J. J. Eriksen, K. Kristensen, T. Kjæegaard, P. Jørgensen, and J. Gauss, J. Chem. Phys. **140**, 064108 (2014).
- ⁸³J. J. Eriksen, P. Jørgensen, J. Olsen, and J. Gauss, J. Chem. Phys. **140**, 174114 (2014).
- ⁸⁴J. J. Eriksen, D. A. Matthews, P. Jørgensen, and J. Gauss, J. Chem. Phys. **143**, 041101 (2015).
- ⁸⁵P. Pulay, Chem. Phys. Lett. **73**, 393 (1980).